www.czasopisma.pan.pl PAN POLSKA AKADEMIA NAUK www.journals.pan.pl

Arch. Metall. Mater., Vol. 61 (2016), No 4, p. 1895–1900

DOI: 10.1515/amm-2016-0305

M. SCENDO*#, N. RADEK**, J. KONSTANTY***, K. STASZEWSKA*

SLIDING WEAR BEHAVIOUR AND CORROSION RESISTANCE TO RINGER'S SOLUTION OF UNCOATED AND DLC COATED X46Cr13 STEEL

Sliding wear properties and corrosion resistance in Ringer's solution of uncoated and diamond-like carbon (DLC) coated X46Cr13 steel was tested. The Raman spectra showed that the DLC film was successfully coated by plasma assisted CVD method onto the steel surface. The wear test, carried out using a ball-on disk tribometer, revealed that the DLC coating show better resistance to sliding wear and lower friction coefficient against a 100Cr6 steel ball than five times softer X46Cr13 steel. The oxidation kinetic parameters were determined by means of both the gravimetric and electrochemical method. It was found that the DLC coating markedly decreased the rate of corrosion of the X46Cr13 steel, irrespective of the corrosion mechanism involved.

Keywords: diamond-like carbon, sliding wear properties, corrosion in Ringer's solution

1. Introduction

The amorphous hydrogenated carbon (HAC) coatings, commonly termed diamond-like carbon (DLC) coatings, have been increasingly applied to tool components and structural parts due to their very attractive mechanical, chemical and electrical properties. DLC coatings are smooth and hard, and provide a large number of advantageous properties. They can be deposited by various chemical and physical vapor depositions techniques e.g. by ion beam deposition, sputtering, cathodic arc evaporation, plasma assisted CVD, plasma based ion implantation and deposition, etc. and find numerous applications [1-3]. DLC is a class of amorphous carbon material that has some properties typical of diamond. It consists of a graphite-like sp^2 bonded carbon embedded in a diamond-like sp^3 bonded matrix and can contain significant amounts of hydrogen. The sp^2 regions have been found to control electronic properties, such as the band gap, while the sp^3 regions are responsible for mechanical properties, such as wear, friction, corrosion resistance, etc. [4]. An optimum combination of the amount of hydrogen, ratio of sp^2 to sp^3 bonding and suitable substrate properties is of key importance to ensure low friction coefficient, high wear resistance, good ductility, adhesion to the substrate and load carrying capability.

DLC coatings can be used to protect materials against corrosion [5]. Amorphous hydrogenated carbon films deposited on steels as protective layers have been used for a variety of applications, including cutting tools and razor blades, and automotive parts, such as piston rings and fuel injectors, etc. [6-9]. Moreover, DLC coatings with low defect density offer an excellent protection against corrosion because they are chemically inert and impermeable [10]. At room temperature DLC can resist chemical attack by practically any acid, alkali or organic solvent. DLC films also demonstrate good biocompatibility and have been found effective as a diffusion barrier in biomedical implants and surgical instruments [11-13]. DLC is generally resistant to destructive attack by body fluids (physiological solutions) and other isotonic liquids including Ringer's solution, invented in the early 1880s by Sydney Ringer, a British physician and physiologist. The solution contains sodium chloride, potassium chloride, calcium chloride, and sodium bicarbonate in concentrations they occur in the body fluids. Ions such as Na^+, K^+, Ca^{2+}, and Mg^{2+} are critical for many functions. Therefore, various Ringer's solutions are products of empirical testing for retention of the activity being studied. Thus recipes provided in this work can serve as a starting point for improved formulations.

2. Experimental

The X46Cr13 grade steel was used as the substrate for deposition of DLC coatings by plasma assisted CVD technique. A steel sample was placed in a plasma chamber, which was subsequently evacuated to a pressure of 1×10^{-4} Pa and backfilled with argon flowing at a rate of 10 sccm. Then plasma was ignited by a non-self-maintained direct current discharge using a hot cathode and anode grid [14]. The voltage between the cathode and anode was set at 400 V, the current through the specimen was 500 mA, and the cathode heating current was 100 A. Following initial argon ion cleaning of the negative biased steel surface, gaseous hydrocarbon (CH_4) was

* JAN KOCHANOWSKI UNIVERSITY IN KIELCE, 15G ŚWIĘTOKRZYSKA STR., 25-406 KIELCE, POLAND
** TECHNICAL UNIV. OF KIELCE, 7 1000-LECIA PANSTWA POLSKIEGO AV., 25-314 KIELCE, POLAND
*** AGH-UNIVERSITY OF SCIENCE & TECHNOLOGY, AL. A. MICKIEWICZA 30, KRAKOW, 30-059, POLAND
# Corresponding author: scendo@ujk.edu.pl

introduced into the plasma chamber at a rate of 50 sccm. The coating process started with an initial attack of film building species and positive ions having energy higher than 2500 eV. The amorphous hydrogenated carbon deposition was continued at a lower ion energy of 180 eV until the final coating thickness of 1.7 μm was reached. The DLC coating was enriched with tungsten in order to increase mechanical properties.

The argon laser Raman spectrometer Jasko NRS -2100 was used to investigate the DLC film. The spectroscopy was performed at room temperature using the 514.5 nm wavelength.

Both uncoated and DLC coated steels were tested for surface topography, Vickers microhardness and friction and wear behaviour using the Joel JSM-5400 scanning electron microscope, Microtech MX3 microhardness tester and HT-1000 ball-on-disk tribotester, respectively. The tribological behaviour was studied in air at room temperature. A fixed 5 mm diameter 100Cr6 steel ball, heat treated to 62 HRC, was used as a counterface. The normal load and sliding velocity were 5 N and 10 m/s, respectively.

Finally the uncoated and DLC coated specimens were subjected to corrosion tests in Ringer's solution by means of the gravimetric and electrochemical method. Analytical purity sodium chloride (NaCl), potassium chloride (KCl) and calcium chloride ($CaCl_2$) were used to prepare the Ringer's solution by dissolving the chlorides in a triple distilled water. The salts were mixed in proportions listed in Table 1. The total concentration of chloride ions and acidity of the solution were 0.159 mol and 5.6 pH, respectively.

TABLE 1

Composition of Ringer's solution

Salt	NaCl	KCl	$CaCl_2$
Mass [g/l]	8.600	0.300	0.480
Concentration [M]	0.147	0.004	0.004

In the gravimetric method the weight loss of three uncoated and three DLC coated steel specimens was determined by weighting them to ± 0.1 mg before and after immersion in 100 cm^3 of corrosive solution at 25°C. Prior to corrosion tests the uncoated steel specimens were ground with #2500 emery paper, washed with bidistilled water, ultrasonically degreased in acetone and dried at room temperature. The corrosion rate was calculated using the formula [15]:

$$v_g = \frac{87.6\,W}{S\,t\,\rho} \tag{1}$$

where: W is the weight loss of the material, S is the specimen surface area, t is the time in corrosive solution, and ρ is the true density of the material.

In the electrochemical method the working (stationary) electrode was made from both uncoated and DLC coated X46Cr13 steel. Its surface area was 2.5 cm^2. Before each measurement the uncoated electrode was also polished with #2500 emery paper, washed with bidistilled water, ultrasonically degreased in acetone and dried at room temperature. A saturated calomel electrode (SCE) and 99.99% platinum foil (1 cm^2) were used as the reference and counter electrode, respectively. The reference electrode was connected with the solution using a Luggin capillary. The capillary tip was positioned 3 mm from the working electrode.

The electrochemical measurements were carried out using the AutoLab PGSTAT 128N potentiostat/galvanostat combined with NOVA 1.7 software. The potentiodynamic polarization curves were recorded at 25±0.5°C within the potential range changing from -900 to +100 mV with a scan rate of 1 mV s^{-1}. The curves were used to evaluate the corrosion potential (E_{corr}) and corrosion current density (j_{corr}) using the Stern and Geary equation:

$$j_{corr} = \frac{b_a\,b_c}{2.303\,(b_a + b_c)}\,\frac{1}{R_p} \tag{2}$$

Substituting

$$B = \frac{b_a\,b_c}{2.303\,(b_a + b_c)} \tag{2a}$$

where b_c and b_a are the Tafel slopes, the polarization resistance can be expressed as:

$$R_p = \frac{B}{j_{corr}} \tag{2b}$$

The corrosion rate of the tested specimens was evaluated using the following equation [16-18]:

$$v_e = 3.268 \times \frac{j_{corr}\,M}{n\,\rho} \tag{3}$$

where: M and ρ are the molecular weight and density of the corroded material, respectively, and n is the number of exchanged electrons.

3. Results and Discussion

Typical Raman spectra of uncoated and DLC coated X46Cr13 steel are shown in Fig. 1. The characteristic DLC spectrum [19], with the main peak at 1430-1480 cm^{-1} corresponding to the graphite-band and a shoulder peak at 1260-1280 cm^{-1} corresponding to the diamond-band, provides clear evidence that the diamond-like film was successfully coated onto the steel surface.

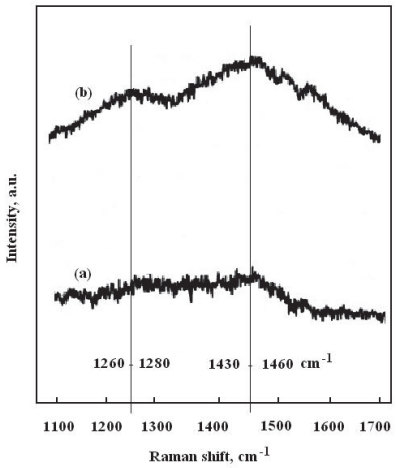

Fig. 1. Raman spectra of: (a) uncoated, and (b) DLC coated X46Cr13 steel

Fig. 2 shows the wear track morphologies on both uncoated and DLC coated steel. The relatively soft (653±5 μHV0.5), uncoated steel was heavily damaged (Fig. 2a) whereas the wear track on the hard (3477±26 μHV0.5) DLC coating was markedly narrower (Fig. 2b), and most importantly, the coating showed good adhesion to the X46Cr13 steel.

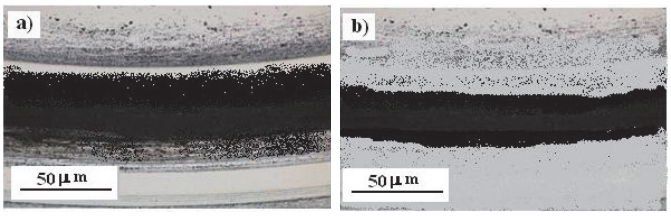

Fig. 2. Wear tracks on: (a) uncoated, and (b) DLC coated X46Cr13 steel

The variation of friction coefficient between the tested specimen and 100Cr6 steel ball with time has been illustrated in Fig. 3. For the X46Cr13 steel and DLC coating the initial values were 0.33 and 0.25, respectively. The friction coefficients increased gradually and stabilized at 0.55 for uncoated steel and 0.38 for DLC coating after about 20,000 and 30,000 cycles, respectively.

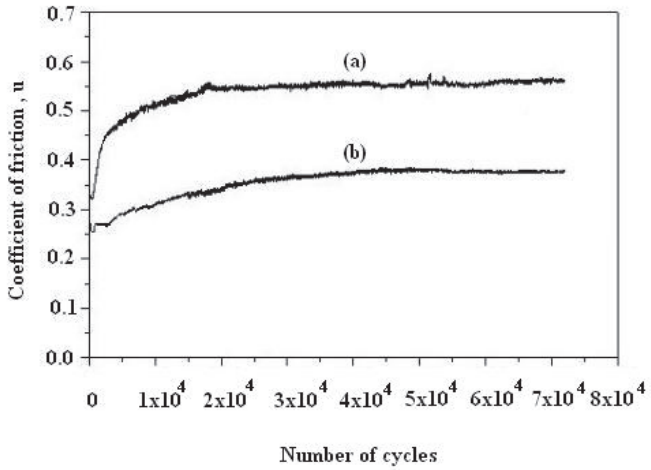

Fig. 3. Coefficient of friction as a function of the number of cycles for: (a) uncoated, and (b) DLC coated X46Cr13 steel

3.1. Corrosion test

The weight loss vs time of immersion curves (gravimetric method) are presented in Fig. 4. The uncoated X46Cr13 steel was dissolving in Ringer's solution very quickly (Fig. 4a). Dissolution of iron in not deoxidized, neutral aqueous chloride solution is a multistage process [20]. Its mechanism can be written as follows:

$$Fe + H_2O + \tfrac{1}{2} O_2 \rightarrow Fe(OH)_2. \quad (4)$$

Then the ferrous hydroxide layer reacts with excess oxygen in the solution, to yield the final corrosion product according to reaction:

$$2\,Fe(OH)_2 + \tfrac{1}{2}\,O_2 \rightarrow \underline{Fe_2O_3} + 2\,H_2O. \quad (5)$$

In acid environment the next reaction is:

$$Fe_2O_3 + 6\,H^+ \rightarrow 2\,Fe^{3+} + 3\,H_2O. \quad (6)$$

In the case of DLC coated steel the oxidation process was markedly slower (Fig. 4b).

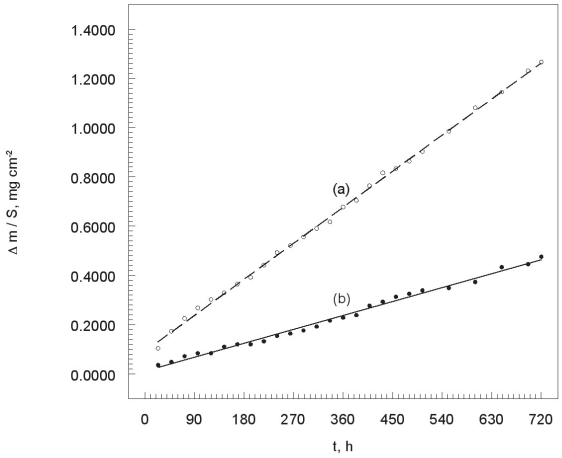

Fig. 4. Corrosion weight loss in Ringer's solution as a function of time for: (a) uncoated, and (b) DLC coated X46Cr13 steel

The corrosion rates for uncoated and DLC coated X46Cr13 steel determined by means of the gravimetric method are summarized in Table 2. It has been found that the DLC coating decreases the rate of corrosion by a factor of three. The corrosion kinetics were studied by fitting the corrosion data to different rate laws [15]. Although the kinetic data may theoretically be interpreted as parabolic, it is well known that the straight line is usually the best fit to experimental data. The considered rate laws were:

$$\text{Zero order: } W_t = k\,t \quad (7)$$

$$\text{First order: } \ln W_t = t + \ln W \quad (8)$$

$$\text{Second order: } 1/W_t = k\,t + 1/W \quad (9)$$

where: W_t is the weight loss after time t of exposure to corrosive environment, and k is the rate constant.

As shown in Fig. 4, the best results, judged by maximizing the coefficients of determination, were obtained for the linear function (7). The results imply that the presence of DLC coating on steel does not change the mechanism of corrosion in Ringer's solution (see reactions (4)-(6)) although it is evident that DLC markedly reduces its rate (Table 3).

Fig. 5 shows the surfaces of X46Cr13 steel and DLC coating prior and after immersion in Ringer's solution for 720 hours. As shown in Figs 5a and 5b, the uncoated steel has been heavily corroded, whereas only a negligible percentage of the

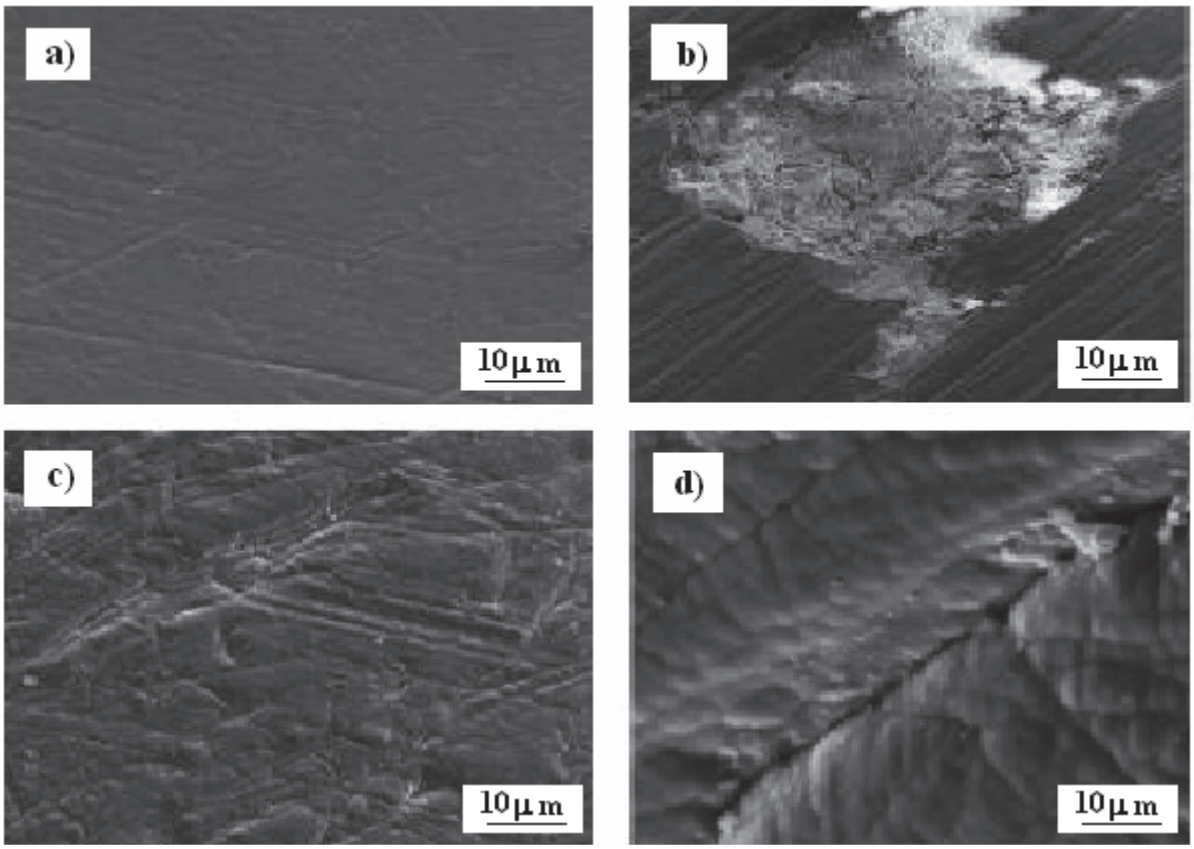

Fig. 5. Surface of X46Cr13 steel (a, b) and DLC coating (c, d), before (a, c) and after (b, d) immersion for 720 hours in Ringer's solution

TABLE 2

Corrosion rates, coefficients of determination, and rate laws calculated for uncoated and DLC coated X46Cr13 steel after immersion for 720 hours in Ringer,s solution at 25 ^{0}C

Materials	υ_g [mm y^{-1}]	R^2	Rate law
Uncoated X46Cr13 steel	0.020	0.9994	Wa = 0.0016 ka + 0.0924
DLC coated X46Cr13 steel	0.007	0.9970	Wb = 0.0006 kb + 0.0113

TABLE 3

Electrochemical corrosion parameters at 25 ^{0}C

Materials	E_{corr} [mV]	j_{corr} [µA cm^{-1}]	$-b_c$	b_a
			[mV / dec]	
Uncoated X46Cr13 steel	-585	5.98	210	140
DLC coated X46Cr13 steel	-437	2.99	270	580

DLC coating has been worn out due to corrosion (see Figs 5c and 5d).

It has been well established that different coatings applied onto a surface of metal (e.g. DLC) may affect the cathodic reactions or anodic reaction or both [21] in electrochemical corrosion testing. The polarization curves for uncoated and DLC coated X46Cr13 steel in Ringer's solution are shown in Fig. 6. The cathode branches correspond to the hydrogen reduction reaction [22-24]. Its mechanism can be described in a simplified form as:

$$Fe + 2\,H^+ \rightarrow Fe + H_2 - 2\,e \qquad (10)$$

The electrolyte was not deoxidized, and the anodic process consisted in dissolution of the steel electrode according to the reactions:

$$2\,Fe + 4\,H^+ + 5/2\,O_2 \rightarrow 2\,FeOOH + H_2O - 4\,e^- \qquad (11)$$

and:

$$2\,FeOOH \rightarrow \underline{Fe_2O_3} + H_2O. \qquad (12)$$

The electrochemical corrosion parameters for the tested materials are listed in Table 3. The positive shift in the E_{corr}

for DLC coated steel is perhaps due to increased effectiveness of cathodic processes as well as decreased rate of anodic reactions. The marked decrease in the corrosion current density (j_{corr}) for DLC coated steel indicates that the coating inhibits attack by chloride ions (0.159 M Cl^-) on the steel surface. Increased values of the cathodic and anodic Tafel slopes (b_c and b_a) indicate that DLC changes the mechanism of electrochemical corrosion. The polarization resistance (R_p) data, evaluated from the slopes of polarization curves, is listed in Table 4. The increasing value of R_p for DLC coated steel shows that the coating retards the exchange of electric charge and mass between the electrode and electrolyte.

TABLE 4

Polarization resistance and corrosion rate at 25 ^{0}C

Materials	R_p [Ω cm^2]	ν_e [mm y^{-1}]
Uncoated X46Cr13 steel	6100	0.069
DLC coated X46Cr13 steel	26750	0.035

Fig. 7 shows chronoamperometric curves obtained at -330 and 50 mV, respectively. The decrease in the current density (curve (a)) was brought about by the formation of a chromium oxide passive layer on the electrode, according to reaction:

$$2\,Cr + 2\,H + 2\,O_2 \rightarrow \underline{Cr_2O_3} + H_2O + . \quad (13)$$

However an increase in the potential to 50 mV brought about a rapid increase in the current density (curve (b)) due to the break-up of the chromium oxide film on the electrode. Hence, the following anodic dissolution of iron can be written as [25]:

$$Fe + Cl^- + H_2O = (FeClOH)_{ads} + H^+ + 2\,e^-. \quad (14)$$

and:

$$(FeClOH)_{ads} + H^+ \rightarrow Fe^{2+} + Cl^- + H_2O. \quad (15)$$

An application of 1.7 μm thick DLC film on the X46Cr13 steel enables a considerable decrease of current density for both cathodic and anodic process (Fig. 6, curve (b)). I is evident, however, that thickness of the coating plays an important role in protecting metals against corrosion in aggressive electrolytes. The 1.7 μm thick DLC film proves insufficient to properly protect the steel surface against corrosion in the chloride environment. It seems clear that by increasing the thickness of the DLC coating (e.g. two times) it should become possible to markedly reduce access of aggressive electrolyte to the steel substrate. Similar conclusions were reached by other authors [26], who discussed the effect of thickness of the DLC layer on CoCrMo alloys. It has been well established [27] that DLC coatings have pinhole-like defects which resemble tiny, needle-like pores. Such defects enable penetration of electrolyte to the substrate, especially at higher polarization potential values (Fig. 6). Although with growing thickness of the DLC coating decreased density of micro-defects in the coating has been observed [28], other problems may arise, such as too high residual stresses which harm adherence of the coating to the metal substrate.

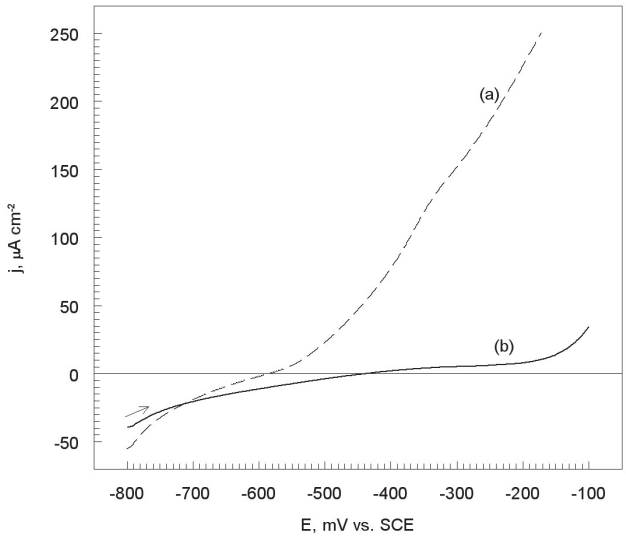

Fig. 6. Polarization curves obtained in Ringer's solution for: (a) uncoated, and (b) DLC coated X46Cr13 steel (dE/dt 1 mV s^{-1}; 25 ^{0}C

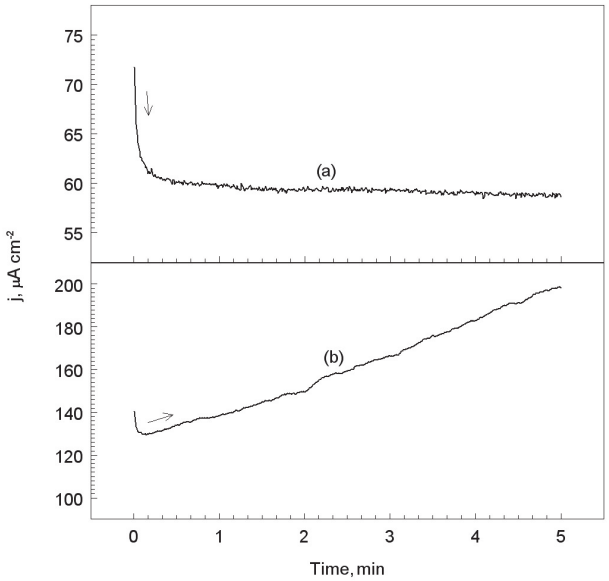

Fig. 7. Chronoamperometric curves obtained at 25^{0}C in Ringer's solution for uncoated X46Cr13 steel at: (a) -330, and (b) 50 mV

4. Conclusions

The experimental work has shown that a 1.7 mm thick DLC coating, correctly applied onto a steel substrate, can impart improved surface mechanical characteristics and resistance to corrosion. The surface properties are mainly manifested by:

1. markedly increased hardness (3477±26 μHV0.5) compared to the X46Cr13 steel substrate (653 ± 5 μHV0.5)
2. greater resistance to sliding wear

3. lower friction coefficient (by approximately 31%) compared to the X46Cr13 steel.

Moreover, the improved resistance to corrosion in Ringer's solution is manifested by:

4. three times slower dissolution of DLC coated X46Cr13 steel
5. limited protection of X46Cr13 steel substrate against electrochemical corrosion. Seemingly insufficient thickness of the DLC coating makes it susceptible to pitting corrosion at a potential increased to approximately 50 mV.

REFERENCES

[1] J. Jiang, R.D. Arnell, J. Tong, Wear **211,** 254-264 (1997).
[2] Y. Liu, E.I. Meletis, Surf. Coat. Technol. 153, 178-183 (2002).
[3] K. Yamaguchi, Y. Wei, I. Horaguchi, Precision Eng. 28, 419-425 (2004).
[4] J. Robertson, Mater. Sci. Eng. R. Rep. 37, 29-281 (2003).
[5] A. Zang, E. Liu, I.F. Annergren, S.N. Tan, S. Zhang, P. Hing, J. Gao, Diamond Relat. Mater. 11, 160-169 (2002).
[6] R.D. Mansano, M. Massi, A.P. Mousinho, L.S. Zambom, L.G. Nato, Diamond Relat. Mater. 12, 749-758 (2003).
[7] S. Sakon, T. Hamada, S. Fujimoto, N. Umesaki, A. Kobayashi, Vacuum **83**, 119-128 (2008).
[8] S.C. Tung, H. Gao, Wear **255**, 1276-1285 (2003).
[9] C.P.O. Treutler, Surf. Coat. Technol. **200**, 1969-1975 (2005).
[10] C. Srividya, S.V. Babu, Chem. Mater. **8**, 2528-2539 (1996).
[11] L.A. Thomson, F.C. Law, N. Ruhston, J. Franks, Biomaterials **12**, 37-44 (1991).
[12] B. Podgornik, J. Vizintin, Surf. Coat. Technol. **200**, 1982-1989 (2005).
[13] J.A. McLaughlin, J.D. Maguire, Diamond Relat. Mater. 17, 873-877 (2008).
[14] A. Dorner-Reisel, C. Schürer, G. Reisel, F. Simon, G. Irmer, E. Müller, Thin Solid. Films 180, 398-410 (2001).
[15] M. Scendo, J. Trela, Int. J. Electrochem. Sci. **8**, 8329-8347 (2013).
[16] M. Scendo, N. Radek, J. Trela, Int. J. Electrochem. Sci. **8**, 9264-9277 (2013).
[17] M. Scendo, J. Trela, B. Antoszewski, T. Kargul, Innovations in Corros. Mater. Sci. **4**, 118-126 (2014).
[18] M. Scendo, J. Trela, N. Radek, Surf. Coat. Technol. **259**, 401-407 (2014).
[19] K. Baba, R. Hatada, Thin Solid. Films 506-507, 55-58 (2006).
[20] E.M. Sherif, Mat. Chem. Phys. **129**, 961-967 (2011).
[21] A.Y. Musa, A.H. Kadheem, A.B. Mohamod, M.S. Takriff, A.R. Daud, S.K. Kamaruddin, Corros. Sci. **52**, 526-533 (2010).
[22] M. Scendo, J. Trela, N. Radek, Corros. Rev. **30**, 33-45 (2012).
[23] M. Scendo, J. Trela, Int. J. Electrochem. Sci. **8**, 9201-9221 (2013).
[24] M Scendo, J. Trela, Int. J. Electrochem. Sci. **8**. 11951-11971 (2013).
[25] R.J. Chin, K. Nobe, J. Electrochem. Soc. **119**, 1457-1461 (1972).
[26] A. Dorner-Reisel, C. Schürer, G. Irmer, E. Müller, Surf. Coat. Technol. **177-178**, 830-837 (2004).
[27] A. Dorner, B. Wielage, C. Schürer, Thin Solid. Films 355, 214-218 (1999).
[28] Z.H. Liu, J.F. Zhao, J. McLaughlin, Diamond Relat. Mater. **8**, 56-65 (1999).